WRDC-TR-89-5052

OPTICAL SPECTROSCOPY OF Ti^{3+} DOPED $YAlO_3$

A. L. Potter
Universal Energy Systems
Dayton, OH 45432

and

K. L. Schepler
Electro-Optics Sources Branch
Electro-Optics Technology Division

AUGUST 1989
Final Report for Period:
June - Aug 1989

Approved for public release; distribution unlimited.

Electronic Technology Laboratory
Wright Reseach and Development Center
Air Force Systems Command
Wright-Patterson Air Force Base, Ohio 45433-6543

NOTICE

WHEN GOVERNMENT DRAWINGS, SPECIFICATIONS, OR OTHER DATA ARE USED FOR ANY PURPOSE OTHER THAN IN CONNECTION WITH A DEFINITELY GOVERNMENT-RELATED PROCUREMENT, THE UNITED STATES GOVERNMENT INCURS NO RESPONSIBILITY OR ANY OBLIGATION WHATSOEVER. THE FACT THAT THE GOVERNMENT MAY HAVE FORMULATED OR IN ANY WAY SUPPLIED THE SAID DRAWINGS, SPECIFICATIONS, OR OTHER DATA, IS NOT TO BE REGARDED BY IMPLICATION, OR OTHERWISE IN ANY MANNER CONSTRUED, AS LICENSING THE HOLDER, OR ANY OTHER PERSON OR CORPORATION; OR AS CONVEYING ANY RIGHTS OR PERMISSION TO MANUFACTURE, USE, OR SELL ANY PATENTED INVENTION THAT MAY IN ANY WAY BE RELATED THERETO.

THIS REPORT IS RELEASABLE TO THE NATIONAL TECHNICAL INFORMATION SERVICE (NTIS). AT NTIS, IT WILL BE AVAILABLE TO THE GENERAL PUBLIC, INCLUDING FOREIGN NATIONS.

THIS TECHNICAL REPORT HAS BEEN REVIEWED AND IS APPROVED FOR PUBLICATION.

Kenneth L. Schepler
Project Scientist
Electro-Optics Sources Branch

Virginia McMillan, Acting Chief
Electro-Optics Sources Branch
Electro-Optics Division

FOR THE COMMANDER:

Richard L. Remski, Chief
Electro-Optics Division
Electronic Technology Laboratory

IF YOUR ADDRESS HAS CHANGED, IF YOU WISH TO BE REMOVED FROM OUR MAILING LIST, OR IF THE ADDRESSEE IS NO LONGER EMPLOYED BY YOUR ORGANIZATION, PLEASE NOTIFY WRDC/ELOS, WRIGHT-PATTERSON AFB, OH 45433-6543 TO HELP MAINTAIN A CURRENT MAILING LIST.

COPIES OF THIS REPORT SHOULD NOT BE RETURNED UNLESS RETURN IS REQUIRED BY SECURITY CONSIDERATIONS, CONTRACTUAL OBLIGATIONS, OR NOTICE ON A SPECIFIC DOCUMENT.

UNCLASSIFIED
SECURITY CLASSIFICATION OF THIS PAGE

REPORT DOCUMENTATION PAGE

Form Approved
OMB No 0704-0188

1a REPORT SECURITY CLASSIFICATION UNCLASSIFIED	1b RESTRICTIVE MARKINGS
2a SECURITY CLASSIFICATION AUTHORITY	3 DISTRIBUTION/AVAILABILITY OF REPORT Approved for public release; distribution unlimited
2b DECLASSIFICATION/DOWNGRADING SCHEDULE	
4 PERFORMING ORGANIZATION REPORT NUMBER(S) WRDC-TR-89-5052	5 MONITORING ORGANIZATION REPORT NUMBER(S)
6a NAME OF PERFORMING ORGANIZATION Wright Research & Development Center 6b OFFICE SYMBOL (If applicable) WRDC/ELOS	7a NAME OF MONITORING ORGANIZATION
6c ADDRESS (City, State, and ZIP Code) Wright-Patterson AFB OH 45433-6543	7b ADDRESS (City, State, and ZIP Code)
8a NAME OF FUNDING/SPONSORING ORGANIZATION 8b OFFICE SYMBOL (If applicable)	9 PROCUREMENT INSTRUMENT IDENTIFICATION NUMBER
8c ADDRESS (City, State, and ZIP Code)	10 SOURCE OF FUNDING NUMBERS PROGRAM ELEMENT NO: 62204F; PROJECT NO: 2001; TASK NO: 05; WORK UNIT ACCESSION NO: 01

11 TITLE (Include Security Classification)

Optical Spectroscopy of Ti^{3+} Doped $YAlO_3$

12 PERSONAL AUTHOR(S)
A. L. Potter and K. L. Schepler

13a TYPE OF REPORT	13b TIME COVERED	14 DATE OF REPORT (Year, Month, Day)	15 PAGE COUNT
Final	FROM 6-89 TO 8-89	89 Aug	35

16 SUPPLEMENTARY NOTATION

This research was performed in cooperation with the AFOSR High School Apprentice Program

17 COSATI CODES			18 SUBJECT TERMS (Continue on reverse if necessary and identify by block number)
FIELD	GROUP	SUB-GROUP	
20	05		Titanium lasers, Ti:$YAlO_3$, fluorescence, nonradiative relaxation, transmission, spectroscopy
20	06		

19 ABSTRACT (Continue on reverse if necessary and identify by block number)

A crystal of titanium-doped $YAlO_3$ grown using the Czochralski method under vacuum conditions was spectroscopically examined. Ti^{3+}:$YAlO_3$ polarized absorbance measurements were made at room temperature. The E||a absorption coefficient was the maximum for the Ti^{3+} peaks at 450 and 500 nm. A large broadband absorption peak at 970 nm was found to be polarized in the E||b orientation. An 840-nm absorption feature changed with crystal location and may be amenable to removal by proper processing. Fluorescence measurements at room temperature showed the typical broadbank peak for Ti^{3+} and produced a pattern of maximum peaks which occurred in the order: E||a at 605 nm, E||c at 608 nm, E||b at 615 nm. Fluorescence measurements at elevated temperatures showed that as temperature increased, peak and integrated intensity decreased. Lifetime measurements of the fluorescence were taken at temperatures ranging from room temperature to 220°C. Lifetime decreased as temperatures increased. A model calculation of lifetime fit to experimental data showed that nonradiative loss in Ti^{3+}:$YAlO_3$ at room temperature was negligible.

20 DISTRIBUTION AVAILABILITY OF ABSTRACT	21 ABSTRACT SECURITY CLASSIFICATION	
☒ UNCLASSIFIED UNLIMITED ☐ SAME AS RPT ☐ DTIC USERS	UNCLASSIFIED	
22a NAME OF RESPONSIBLE INDIVIDUAL K. L. Schepler	22b TELEPHONE (Include Area Code) (513) 255-2804	22c OFFICE SYMBOL WRDC/ELOS

DD Form 1473, JUN 86 Previous editions are obsolete

SECURITY CLASSIFICATION OF THIS PAGE

The Heraeus crystal has optical properties quite similar to the Airtron crystals studied earlier. It does have larger size and better optical quality. But scattering and absorption loss in the fluorescence spectral region are still present in this sample. The region of fluorescence (and potential lasing) makes this an interesting material. However, its potential as a laser material requires further investigation of its gain, loss, and excited state absorption properties.

FOREWORD

This report describes the results of research performed under the auspices of the Air Force Office of Scientific Research High School Apprenticeship Program at WRDC/ELOS. Technical effort was performed by Ms A. Potter. Dr K. L. Schepler was her mentor and program manager. Lt R. Oliver and Mr R. Wade assisted with data acquisition and analysis. Supply of a $Ti^{3+}:YAlO_3$ crystal sample by Dr R. Simms of the Naval Air Development Center is gratefully acknowledged.

TABLE OF CONTENTS

LIST OF ILLUSTRATIONS

I. INTRODUCTION

This project investigated the optical properties of $Ti^{3+}:YAlO_3$ and its potential as a laser material. A large single crystal sample grown by Heraeus was provided by R. Simms of the Naval Air Development Center for investigation. Prior $Ti^{3+}:YAlO_3$ crystals investigated in this lab had been grown by Litton Airtron, but they showed large amounts of scattering and absorption loss in the fluorescence part of the spectrum. Since Heraeus used a different method for growing $Ti^{3+}:YAlO_3$ (growth under a vacuum), we wanted to see if this crystal might be a better material for lasing. Absorbance, fluorescence, annealing, and lifetime measurements were performed.

The crystal of $Ti^{3+}:YAlO_3$ was grown by Heraeus in West Germany by using the modified Czochralski method under stringent vacuum conditions. It was 0.1 atom percent (at%) Ti by melt and had a beige-orange tint. The crystal dimensions were 1.026 cm by 1.509 cm by 3.05 cm (see figure 1). A rectangular parallelepiped of size 0.3 cm by 1.026 cm by 1.01 cm was cut from the original crystal. The sample faces were cut perpendicular to crystallographic axes. The crystal had surface imperfections on the bc faces which appeared to be laser damage spots.

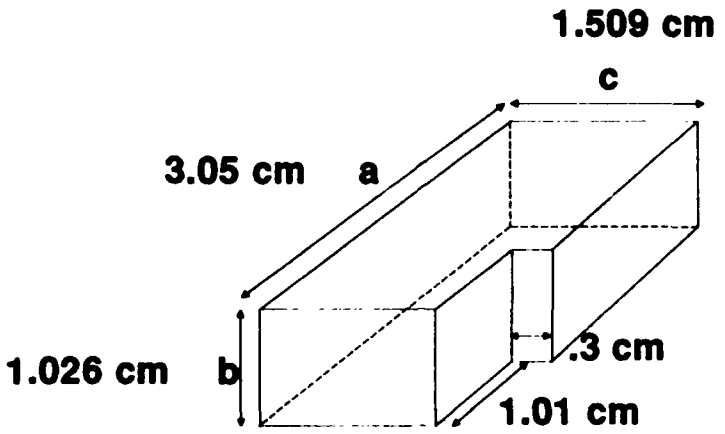

Figure 1. Diagram of the Ti:$YAlO_3$ Crystal

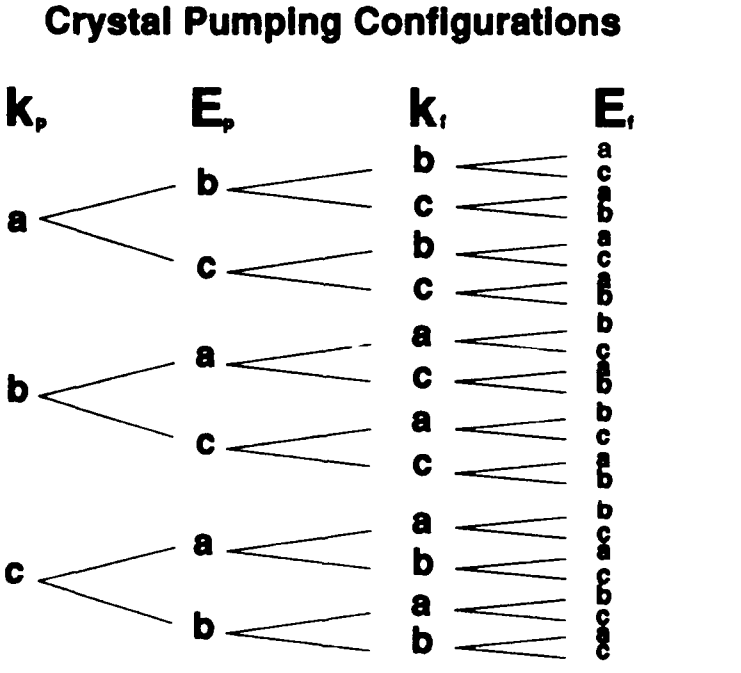

Figure 2. Possible polarization combinations.

II. EXPERIMENT

Absorption Measurements

An IR9 Spectrophotometer with a polarizer/depolarizer unit, made by Perkin-Elmer, was used to measure polarized transmission in the crystal at the six possible combinations of polarization and beam direction (e.g. E$\parallel$a and k$\parallel$c or k$\parallel$b; E$\parallel$b and k$\parallel$a or k$\parallel$c; E$\parallel$c and k$\parallel$a or k$\parallel$b; where E = the electric field and k = beam direction). Transmission scans were taken from 300 nm to 2000 nm in increments of 1 nm.

An annealing experiment was carried out by baking the crystal for 15 hours in an oven at 200°C exposed to the atmosphere. The absorption spectra were measured again with the spectrophotometer to see if the broadband peak around 800-1000 nm or the amount of scatter would change in any way.

Fluorescence Measurements

Polarized fluorescence measurements were taken to further investigate the optical properties of this crystal. Fluorescence scans of intensity versus wavelength at room temperature were recorded with the crystal in the twenty-four possible combinations of pump beam polarization, pump beam direction,

fluorescence polarization, and fluorescence direction (see figure 2). The laser beam pumping the crystal and the fluorescence entering the spectrometer were both polarized. The slits in the Spex 1.26 meter spectrometer were set at 50 μm. A Spectra Physics 165 argon ion laser was used to optically pump the crystal at a power of 500 mW. Two pump wavelengths of 488 nm and 514.5 nm were used in the experiment. Each run was a scan between 500 and 800 nm with increments of 1 nm. The wavelength was calibrated using emission lines from a standard krypton lamp (see Appendix 1). Fluorescence was recorded using a Hamamatsu R928 photomultiplier tube (PMT). Spectral response of the spectrometer was corrected using previously recorded tungsten lamp (black body) calibration runs. Fluorescence polarization was selected using a standard polaroid film and a depolarizer was placed behind it to remove any polarization-dependent sensitivities in the spectrometer.

Fluorescence Lifetime Measurements

Measurements of fluorescence lifetime versus temperature were performed. In these measurements accurate temperature monitoring was accomplished by comparing temperatures measured by a calibrated thermometer to two thermocouples. One thermocouple was connected to a Cole-Parmer Digi-Sense Model 2168-80

Temperature Controller and the other was connected to a Bailey Instruments Co., Inc. Wide Range Thermometer (Model BAT-7). The comparison was done by placing thermocouples, connected to each monitor, and the thermometer into a beaker of oil heated up to 220°C (according to the thermometer). Temperatures of the three temperature meters were recorded and are shown in figure 3. This graph was used to correct thermocouple readings to true temperatures in data plots.

The $Ti^{3+}:YAlO_3$ crystal was mounted on a copper block in a vacuum oven. The temperature controller's thermocouple was attached to the top of the crystal. The controller also supplied current to a heating element in the copper block, and an air pump cooling system was used to provide better temperature control. A second thermocouple was mounted inside the copper block and was monitored by the wide range thermometer. Measurements of fluorescence lifetime were made at room temperature (20°C) and at approximately 50° increments up to 220°C. A Hastings Vacuum Gauge, model VT-4S2, measured a vacuum of 0.7 mm of mercury in the sample chamber.

For the lifetime measurements, the argon ion laser was operated at 488 nm with a power of 1 W. An acousto-optical switch was used to select pulses from the beam that were 100 μs long and had rise and fall times (10%-90%) of 1-2 μs. The fluorescence was detected at 600 nm with the R928 PMT. PMT

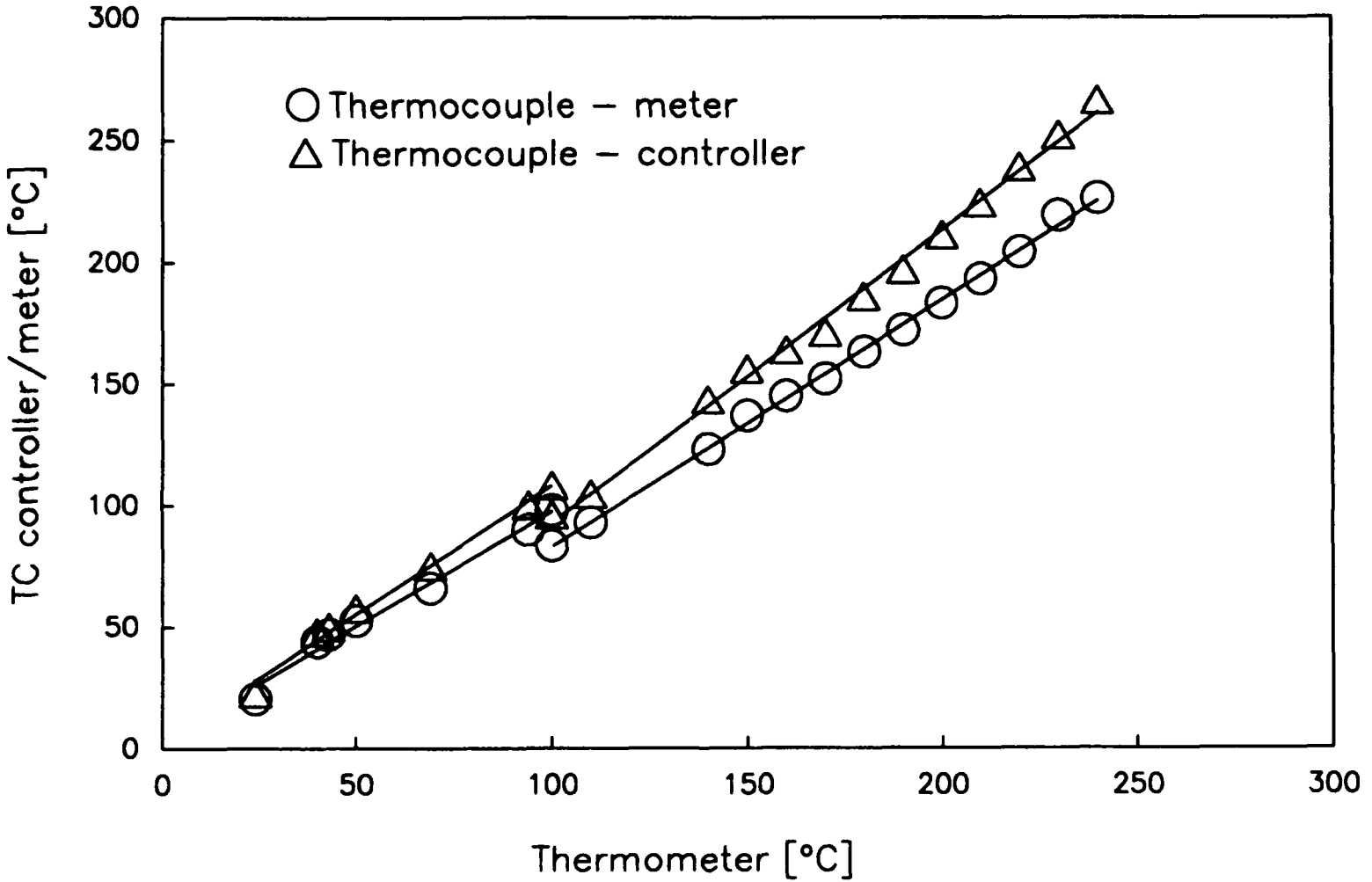

Figure 3. Thermocouple calibration measurements. Lines are least square fits.

signals were recorded every 40 ns using a LeCroy 3500SA digitizer and signal averaged for 1000 pulses.

Further fluorescence scans were made as a function of temperature in the 20-235°C range. The argon ion pump laser was operated at 488 nm with 100 mW of power. The slits on the spectrometer were set at 300 μm and the spectrometer took data in increments of 1 nm.

III. RESULTS AND DISCUSSION

Calculation of Absorption Coefficient

The results of the transmission measurements were manipulated to calculate the absorption coefficient using these two equations:

$$T = I/I_0 = e^{-(\alpha l)} \qquad (1)$$

$$T = I/I_0 = 10^{-x} \qquad (2)$$

where x = absorbance measured by the instrument, l = crystal thickness or beam pathlength, T = transmission, I = intensity, I_0 = incident intensity and α = absorption coefficient. Taking the natural log of both equations gives,

$$-\alpha l = -x(\ln 10) \qquad (3)$$

or

$$\alpha = x(\ln 10)/l \qquad (4)$$

Using equation 4 removes the effect of different path lengths (different crystal thicknesses) to yield the absorption coefficient (α).

But before using eq. 4, a correction for Fresnel losses (reflection losses) had to be made. The reflection loss was determined by first calculating how much of the beam is reflected when it hits the first face of the crystal. This is calculated using the formula,

$$R = (n_0-n_1)^2/(n_0+n_1)^2 \qquad (5)$$

where n_0 = refractive index of the atmosphere, n_1 = refractive index of $Ti^{3+}:YAlO_3$ ($E\|a$ n_1 = 1.97; $E\|b$ n_1 = 1.96; $E\|c$ n_1 = 1.94). The parameter R is the fraction of light reflected from the first face. The same fraction of the beam is reflected back into the crystal when the beam strikes the second face of the crystal. The light transmitted out of the second surface is $(1-R)^2$. Since $R \ll 1$, further bounces need not be considered. The negative log of this decimal fraction is subtracted from the absorbance in order to remove reflection losses (see figure 4 for

$$R = (n_1 - n_2)^2 / (n_1 + n_2)^2$$

n_1 = refractive index of air

n_2 = refractive index of $YAlO_3$

Ella = 1.97
Ellb = 1.96
Ellc = 1.94

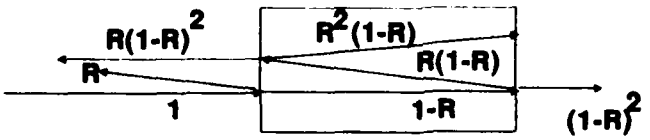

Diagram of a laser beam going through the TI:YAlO crystal

$R(\text{Ella}) = (1-1.97)^2 / (1+1.97)^2 = .1067$
$= 10.67\%$

$(1-R)^2 = .798$

Fresnel Loss = -log(.797) = 0.098

True Absorbance = measured absorbance - 0.098

Figure 4: An example of Fresnel Loss Calculation

a calculation example). This value can then be used as the true absorbance (x) to find the absorption coefficient (α).

Absorption Coefficient Graphs

Absorption spectra of $Ti^{3+}:YAlO_3$ showed a pair of peaks at 450 nm and 500 nm (see figure 5). These peaks are characteristic of Ti^{3+} absorption[1] but they are at shorter wavelengths than Ti^{3+}:sapphire peaks indicating that $Ti^{3+}:YAlO_3$ has a larger crystal field at the titanium site. Absorption increased rapidly for wavelengths shorter than 370 nm in the ultraviolet region. Between 700 and 1100 nm several features were observed. First, there was a weak and extremely broad absorption band in the near-infrared region peaking around 840 nm for the E$\parallel$c and E$\parallel$a polarizations in figure 5. A stronger broadband absorption peak was observed for E$\parallel$b peaked at 970 nm. Very weak but sharp features in the 650, 750, and 800-nm regions were probably small amounts of Nd^{3+} contamination.

The E$\parallel$a axis had the greatest Ti^{3+} absorption but it also had the greatest amount of background loss in the UV-visible region. The Ti^{3+} peak magnitudes were unique for each crystal axis. The 450-nm peak was greater than the 500-nm peak in the E$\parallel$a and E$\parallel$c orientations, but the 500-nm peak was greater for the E$\parallel$b orientation.

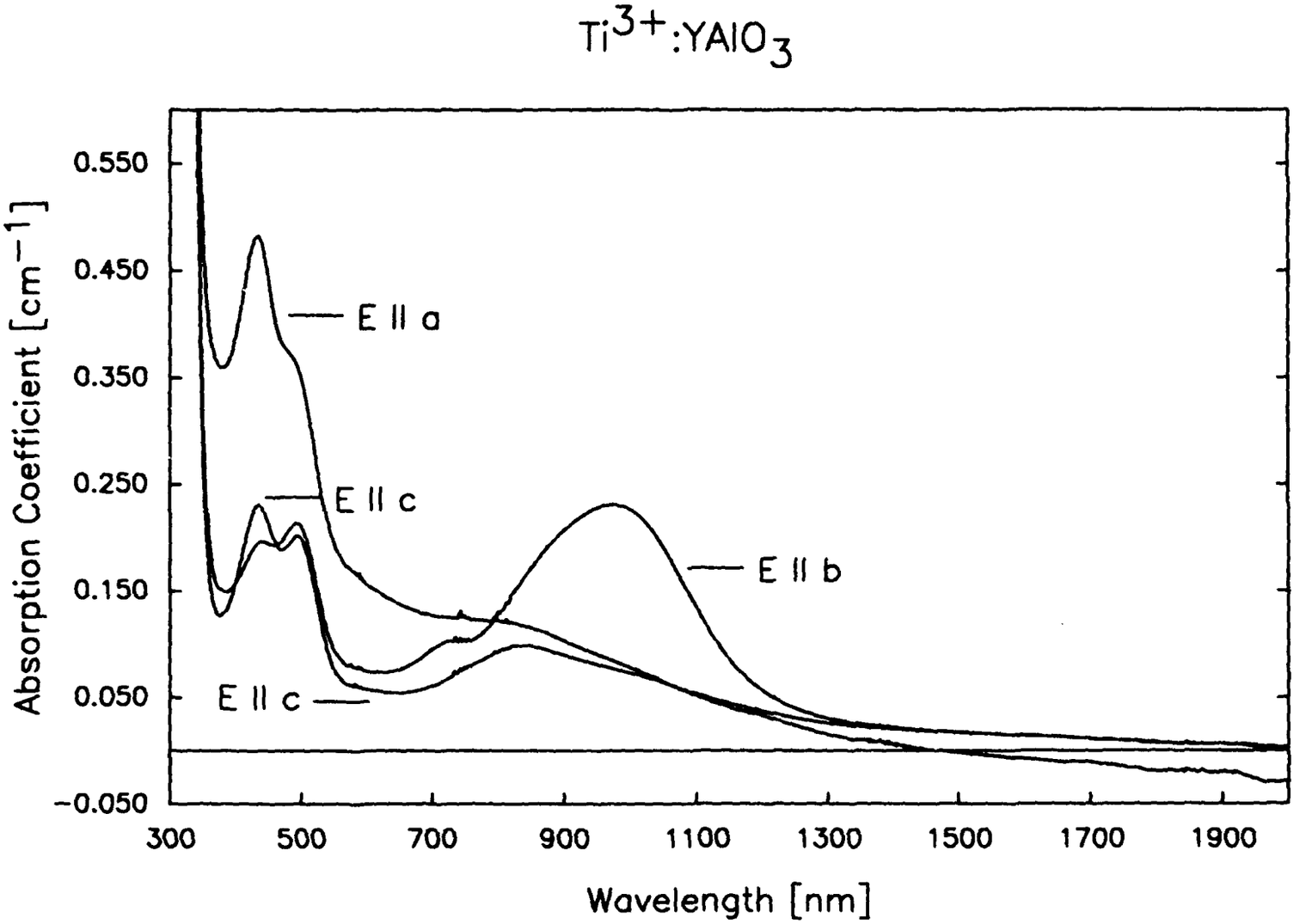

Figure 5. Polarized absorption spectra.

The polarized absorption features are similar to those observed by Moulton[2] except for a permutation of crystal axes and differences in relative amounts of IR absorption and scattering at all wavelengths. Moulton's 'a_M' axis corresponds to our 'c' axis, 'b_M' corresponds to our 'a' axis, and 'c_M' corresponds to our 'b' axis. In both cases we are depending on results of x-ray measurements provided by the grower (Airtron for Moulton, Heraeus for us) so we cannot determine which axis assignment is correct.

The samples examined by Moulton had higher titanium doping concentrations than the Heraeus sample so comparisons of relative magnitudes is enlightening. The 450 and 500-nm peaks scale well with at% titanium doping. The 970-nm peak also scales linearly with titanium doping indicating that its presence is directly related to the presence of titanium ions in the host. The IR peak near 840 nm does not scale with titanium concentration; it is much smaller in the Heraeus sample. It also varied in magnitude for scans where the crystal position was changed. Thus the 840-nm peak appears to be amenable to removal when vacuum growth is used.

$Ti^{3+}:YAlO_3$ Crystal Annealed

In the spectra that were done after the annealing experiment, only one changed dramatically. That spectrum, with E$\|$a and k$\|$b

(k is the propagation direction), had noticeably less loss at all wavelengths and the broadband 840-nm peak decreased in height. The high temperature anneal appeared to have removed some color center or defect from the crystal.

To determine whether the effect was due to the annealing or simply differences in transmission in different parts of the crystal, absorption scans were made by translating the crystal perpendicular to the beam by small amounts from run to run (see figure 6). All of the runs had very similar Ti^{3+} peaks indicating uniform doping. The broadband features in the 700-1100 nm region were not constant from run to run. The differences in baseline absorption increased with increasing wavelength due, most likely, to differences in the amount of scattering present at different sites.

Next, a 633-nm helium-neon laser beam was passed through the crystal. The crystal was moved so that the laser beam passed through different areas of the crystal. Cloudy areas with large beam scatter were observed near the crystal surfaces. The interior produced a very low amount of scatter. Thus the observed annealing experiment changes were probably artifacts of changes in the beam position rather than any annealing effects.

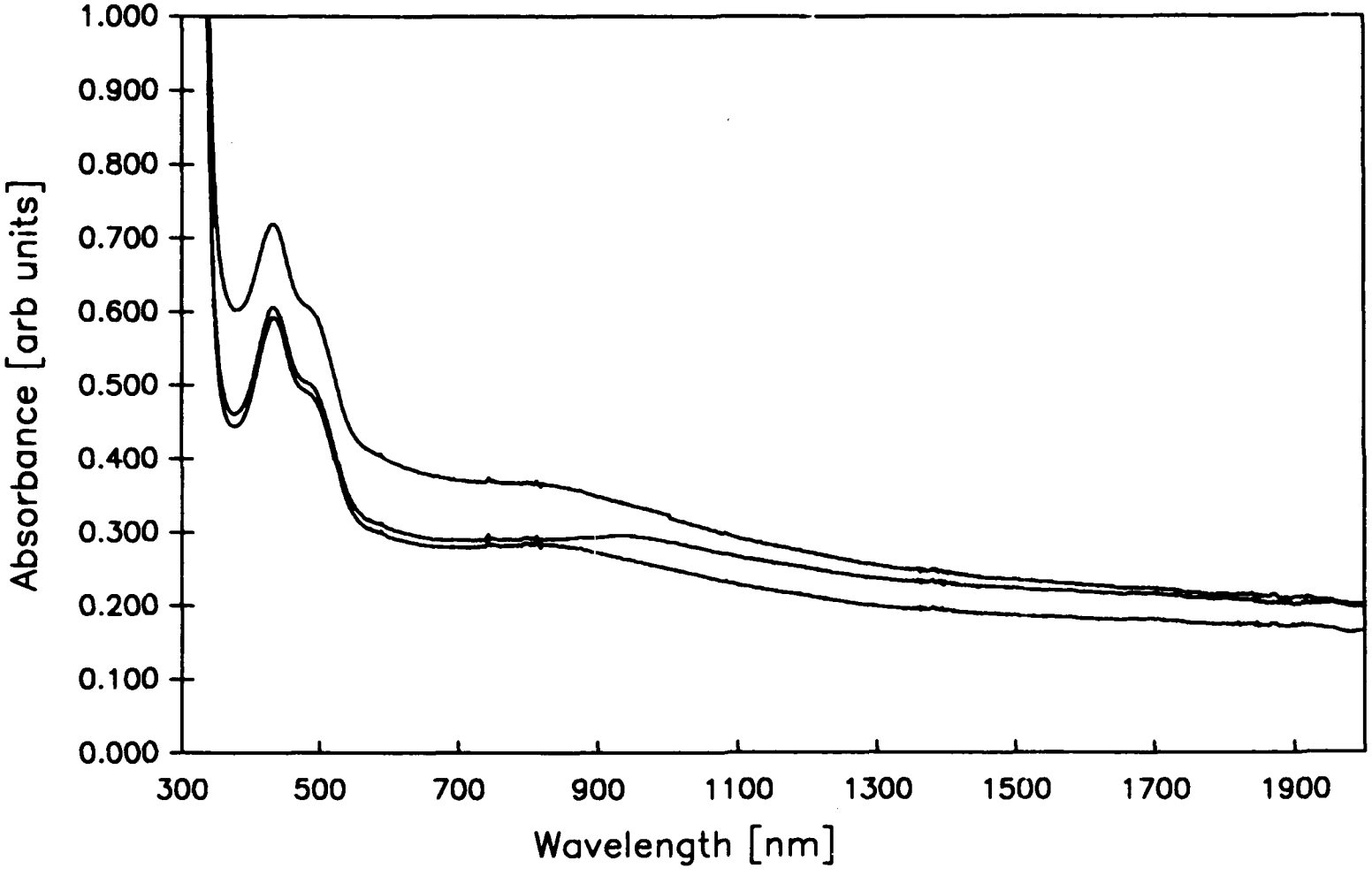

Figure 6. Ella Ti^{3+}:$YAlO_3$ loss at 3 points in the sample; no reflection corrections.

Fluorescence Measurements at Room Temperature

The results of the fluorescence measurements at room temperature showed the broadband single peak typical of Ti^{3+} ions. The polarized fluorescence spectra shown in figure 7 have been corrected for spectrometer response and are to scale relative to one another. Where E is the electric field of the fluorescence, E||a fluorescence peaked at 605 nm, E||c fluorescence peaked at 608 nm, and E||b fluorescence peaked at 615 nm. The sharp peak near 590 nm was probably a grating ghost since it disappeared when the pump wavelength was changed. The relative polarized fluorescence intensities increased in the order a:c:b. Although the differences are minor, the relative intensities did not agree with those observed using an Airtron-grown sample.[1]

Fluorescence and Lifetime Measurements at High Temperatures

The fluorescence measurements at high temperatures showed that the intensity peak of the unpolarized fluorescence decreased with increasing temperature (see figure 8). The intensity decreased to 49% of its room temperature value when the temperature was increased to 222°C. The integrated intensity was also found by summing up the recorded intensities at each increment between 500 and 800 nm. It showed an almost identical

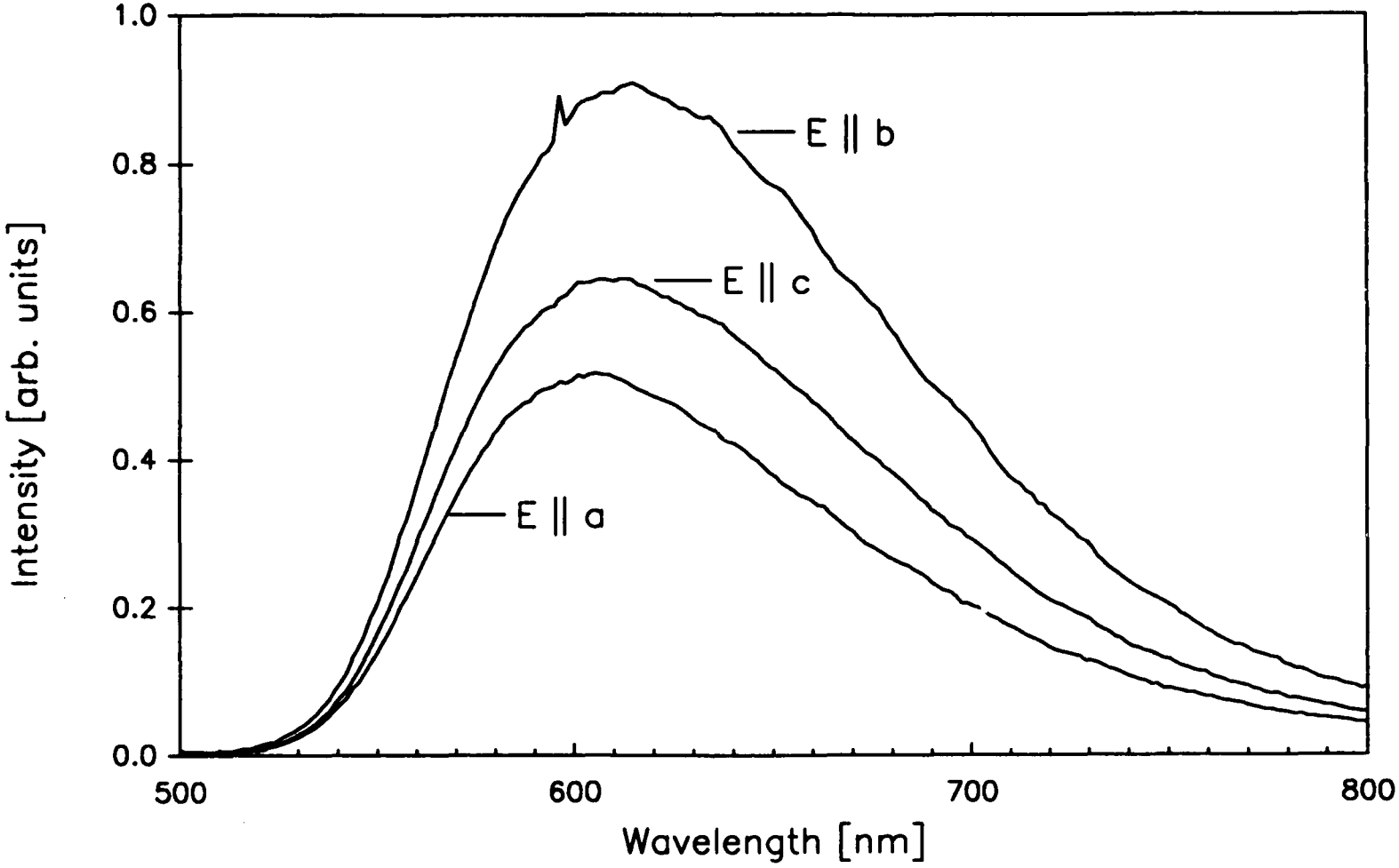

Figure 7. Ti^{3+}:$YAlO_3$ polarized room temperature fluorescence.

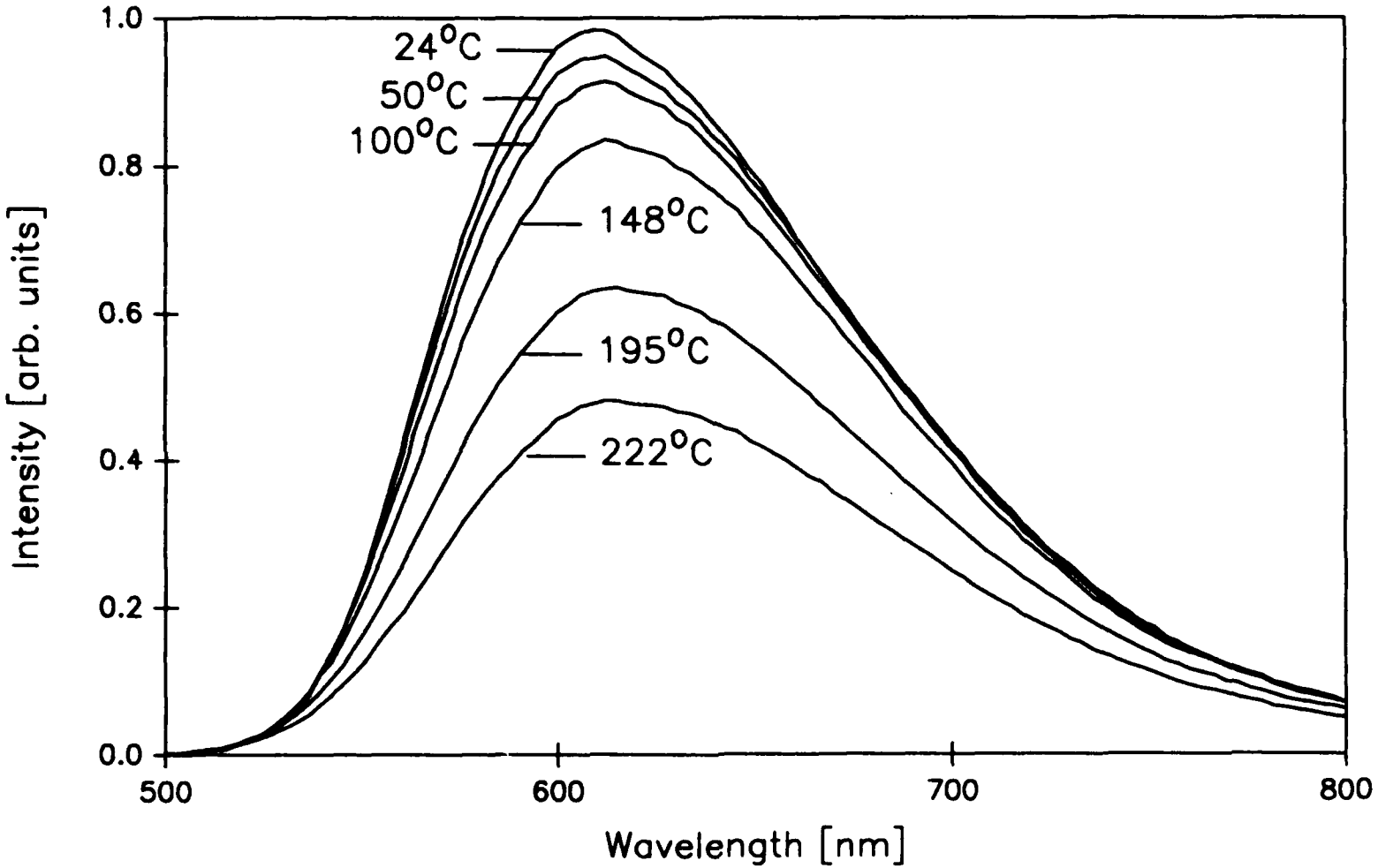

Figure 8. Ti^{3+}:$YAlO_3$ fluorescence at elevated temperatures.

decrease with temperature since the width of the peak changed little in this temperature range.

Assuming single exponential decay, the equation of fluorescence intensity as a function of time after an initial excitation pulse is given by

$$I = I_0 e^{-t/\tau} \qquad (6)$$

where I_0 = the intensity at time = 0, t = time and τ = lifetime. Taking the natural log of both sides of eq. 6 results in

$$\ln(I) = \ln(I_0) - t/\tau \quad . \qquad (7)$$

When the following substitutions are made: ln I = y; ln I_0 = mx; $-t/\tau$ = b, this equation can be recognized as the equation for a straight line, i.e.,

$$y = mx + b \quad . \qquad (8)$$

Lifetimes were calculated by finding the least-squares fit to the slope of the log of the intensities. Graphs of intensity versus time and log(intensity) versus time are shown in figure 9 for two temperatures. The constant intensity for the first 12 μs shows the steady state emission during the pump pulse. Once the pump power is turned off, the fluorescence decays exponentially. The constant slopes of the semilog plots show that the

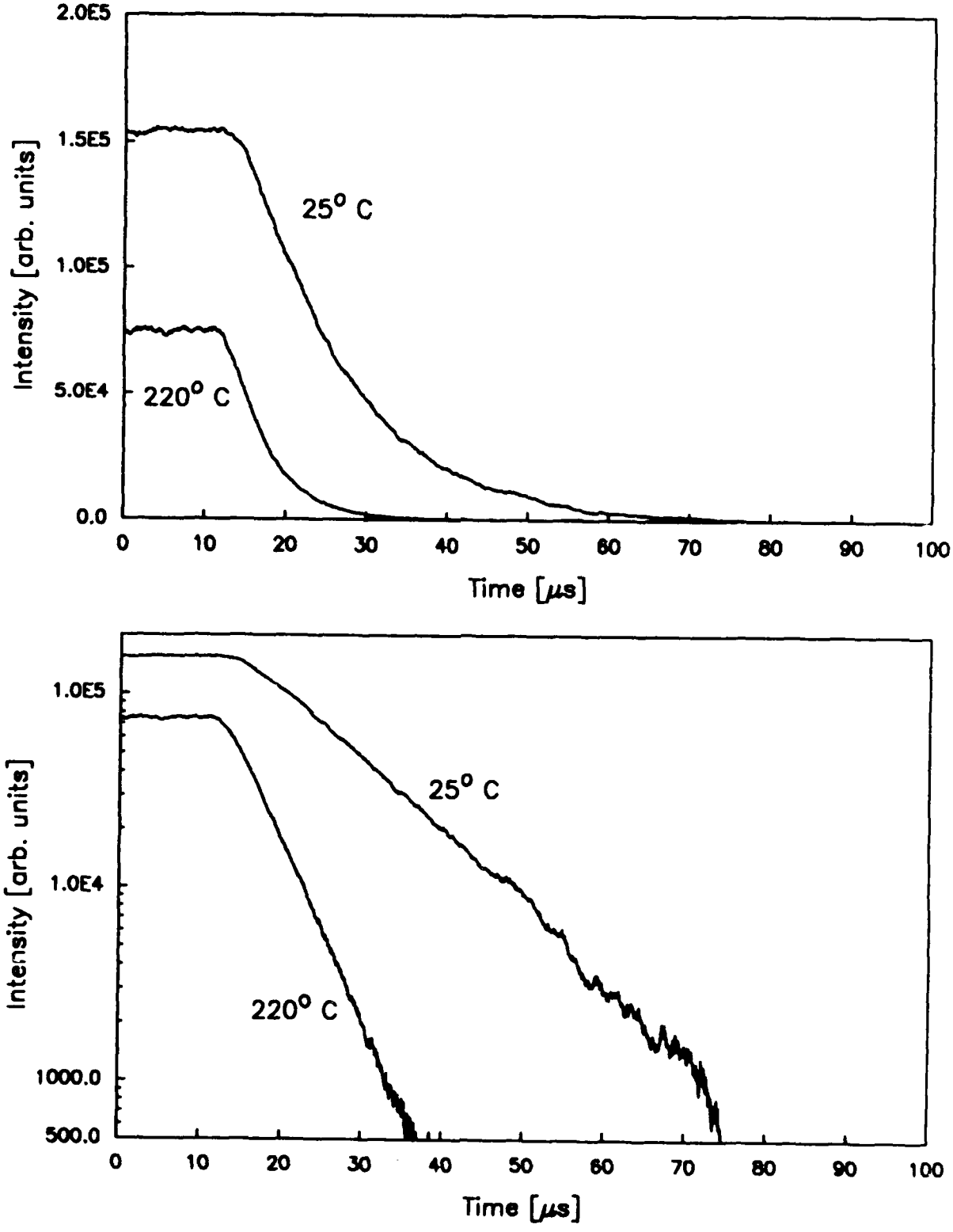

Figure 9. Ti^{3+}:YAlO, fluorescence versus time.

fluorescence is well described by a single exponential decay. The single exponential decay indicates that all of the Ti^{3+} ions are located in similar sites. Location in more than one type of site would result in more than one characteristic lifetime and a nonlinear semilog plot.

In these graphs the lifetime can be compared on the basis of slope; the steeper the slope the shorter the lifetime. The lifetime was found to decrease as temperatures increased similar to the integrated intensity values except that the lifetime decreased at a faster rate. Figure 10 shows a plot of lifetime and integrated intensity rates versus temperature. Lifetime at room temperature was 12.4 μs and decreased to 4.8 μs at 220°C.

Figure 11 shows a calculation of lifetime based on Struck and Fonger methods[3] compared to measured lifetimes. Although the model has parameters which were adjusted to fit the data, the parameter values were very similar to those used to fit other titanium-doped hosts. The main difference was the presence of a larger crystal field splitting in $Ti^{3+}:YAlO_3$. The crystal field used in the model was based on a previously observed zero-phonon peak at 540 nm. An excellent fit of model calculations to measured lifetimes was achieved using the following parameter values:

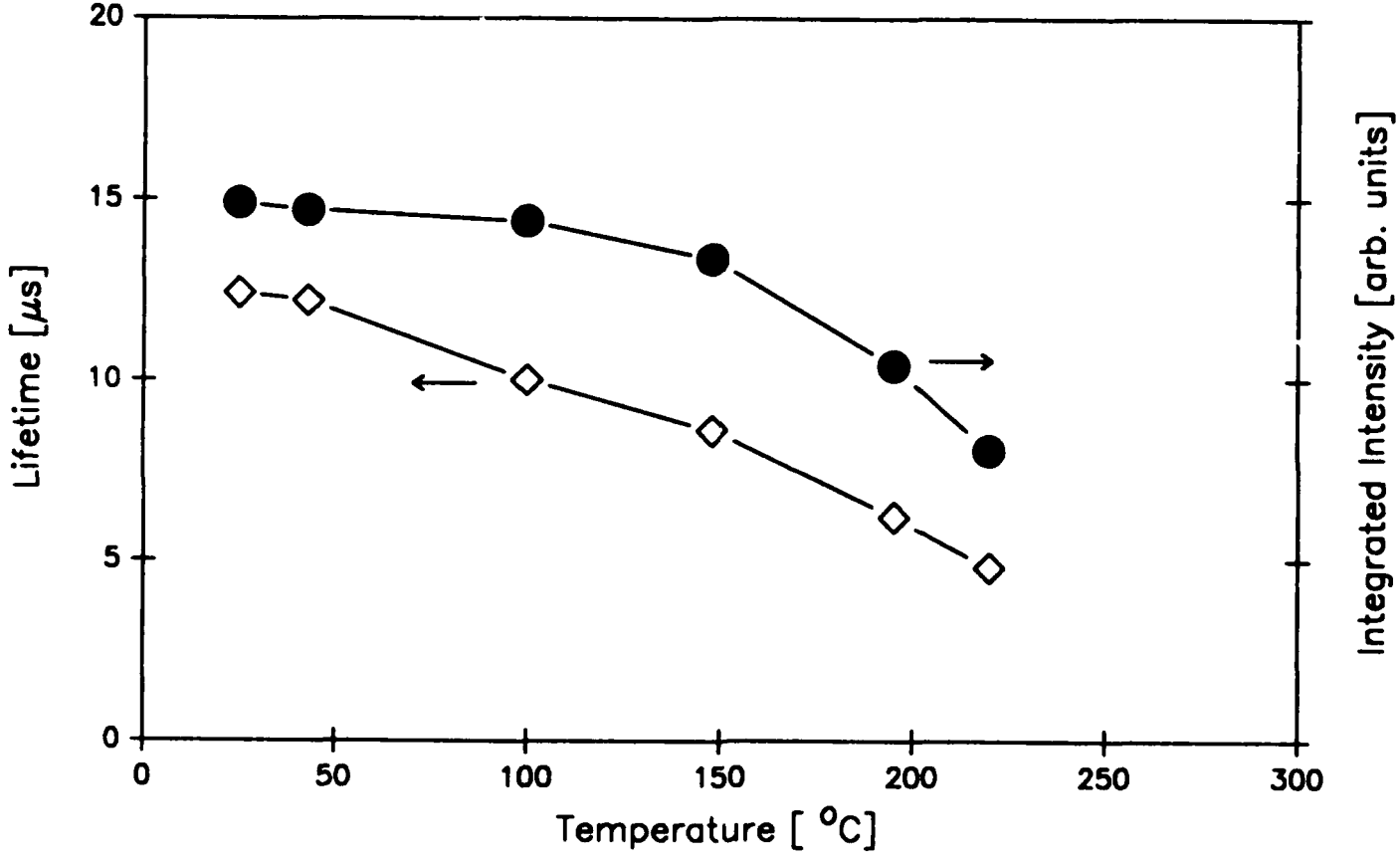

Figure 10. High temperature Ti^{3+}:$YAlO_3$ lifetime and integrated intensity.

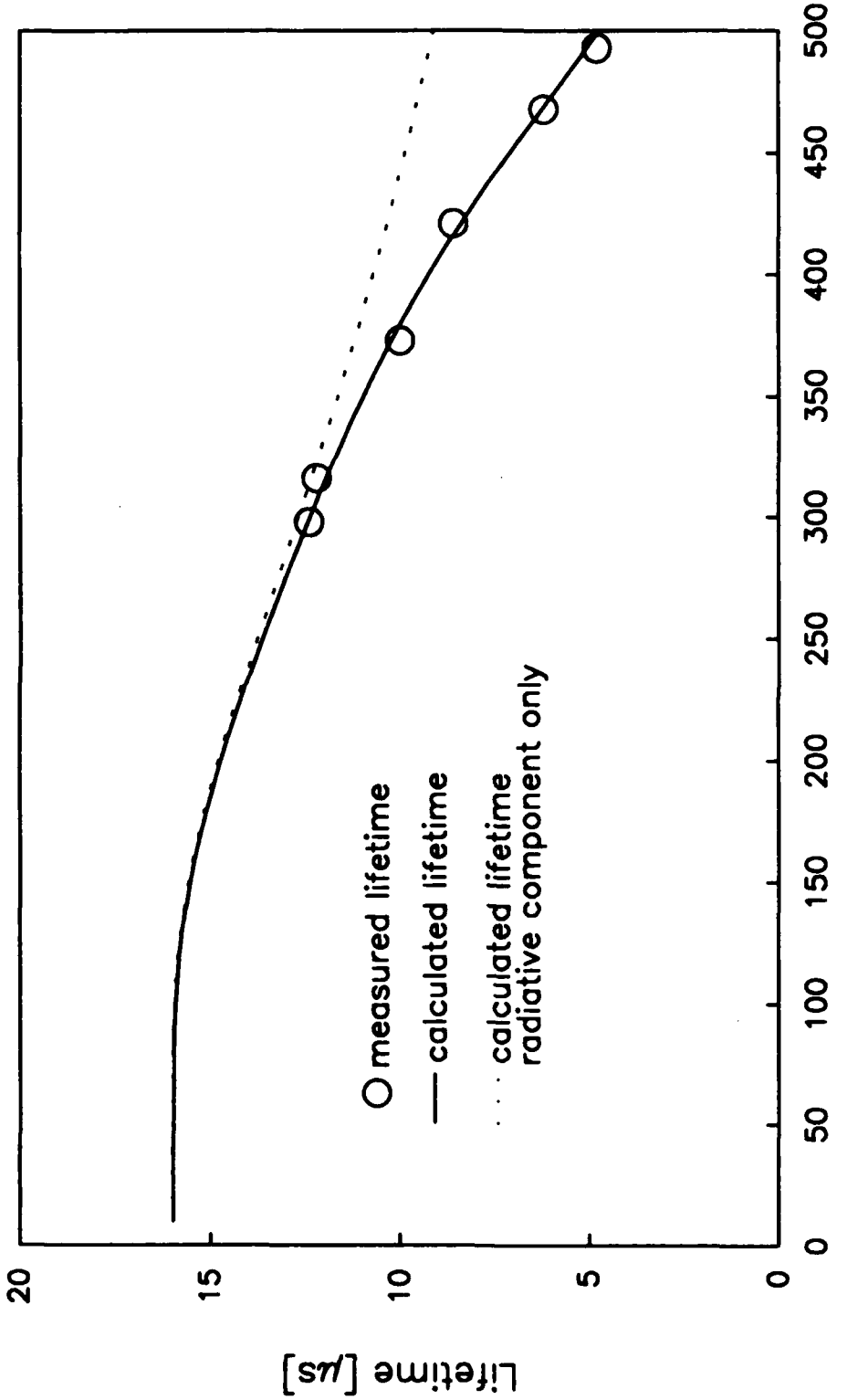

Figure 11. Ti^{3+}:$YAlO_3$ lifetime fit to model calculations.

Stokes shift:	10.2
phonon energy:	450 cm^{-1}
τ_{vib}:	16 μs
τ_{rad}:	large
N (nonradiative rate constant)	5.0×10^{14} Hz

Complete definitions of these parameters may be found in AFWAL-TR-88-1125. The plot of figure 11 also shows the expected change in lifetime if no nonradiative loss were present (the dotted line). Clearly, nonradiative loss is present but its effects are small until very high temperatures are reached. Quantum efficiency at 300 K (room temperature) is calculated to be 98.6% and only drops off to 52% at 500 K. Thus $Ti^{3+}:YAlO_3$ should have negligible nonradiative loss for laser applications.

IV. SUMMARY

$Ti^{3+}:YAlO_3$ polarized absorbance measurements were taken at room temperature. The E||a absorption coefficient was the maximum for the Ti^{3+} peaks at 450 and 500 nm. A large broadband absorption peak at 970 nm was found to be polarized in the E||b orientation. An 840-nm absorption feature changed with crystal location and may be amenable to removal by proper processing.

Fluorescence measurements at room temperature showed the typical broadband peak for Ti^{3+} and produced a pattern of maximum peaks which occurred in the order : E||a at 605 nm, E||c at 608 nm, E||b at 615 nm. Fluorescence measurements at elevated temperatures showed that as temperature increased, peak and integrated intensity decreased. Lifetime measurements of the fluorescence were taken at temperatures ranging from room temperature to 220°C. Lifetime decreased as temperature increased. A model calculation of lifetime fit to experimental data showed that nonradiative loss in $Ti^{3+}:YAlO_3$ at room temperature is negligible.

The Heraeus crystal has optical properties quite similar to the Airtron crystals studied earlier. It does have larger size and better optical quality. But scattering and absorption loss in the fluorescence spectral region are still present in this sample. The region of fluorescence (and potential lasing) makes this an interesting material. However, its potential as a laser material requires further investigation of its gain, loss, and excited state absorption properties.

REFERENCES

1. K.L. Schepler, "Spectroscopy and Laser Performance of Ti^{3+} Doped and Cr^{3+},Nd^{3+} Co-doped Crystals," AFWAL-TR-88-1125, Aug. 1988.

2. Peter F. Moulton, "An investigation of Ti:$YAlO_3$ as a tunable laser material," Final Report for Office of Naval Research, Contract N00014-85-C-0533, Aug 1987.

3. C.W. Struck and W.H. Fonger, J. of Lumin. 10, 1 (1975).

APPENDIX

Wavelength Calibration using a Krypton Lamp

Krypton lamp scans were first carried out to calibrate wavelength for fluorescence measurements using the SPEX 1269 Spectrometer and a 1200-g/mm grating blazed at 750 nm. The controller used with the spectrometer was a SPEX Datamate DM1 controller. Wavelength calibration was done by making several scans of the krypton lamp spectrum. All of the scans were done in the range of 500 to 800 nm. Two different types of scans were used. The first used a PIN silicon detector made by United Detector Technologies, Inc. and the second used a Hamamatsu R928 photomultiplier tube .

Next, the grating was changed so shorter wavelength fluorescence could be measured. Again wavelength was calibrated for fluorescence measurements using the SPEX 1269 Spectrometer and a 1200-g/mm grating blazed at 400 nm. Scans were made between 400 nm and 800 nm with the R928 photomultiplier tube. The slit size was 10 μm and data was taken at increments of 0.2 Å.

TABLE 1
TABLE OF λ's FOR 750 NM BLAZE GRATING

1) Main peaks found with the silicon detector, 1 mm slits, and increments of 1 Å

EXPECTED PEAKS(Å)	MEASURED PEAKS(Å)	OFFSET(Å)
5570.3	5573.	2.7
5870.9	5874.	3.1
7587.4	7590.	2.6
7601.5	7604.	2.5
7685.2	7688.	2.8
7694.5	7697.	2.5
	Average Offset =	+2.7

2) Main peaks found with the PMT, 100 μm slits, and increments of .01 Å (measured peaks rounded to one decimal place.)

EXPECTED PEAKS(Å)	MEASURED PEAKS(Å)	OFFSET(Å)
5570.3	5571.9	1.6
5870.9	5872.6	1.7
7587.4	7588.9	1.5
7601.5	7603.1	1.6
7685.2	7686.8	1.6
7694.5	7696.2	1.7
7854.8	7856.6	1.8
	Average Offset =	+1.6

3) Main peaks found with the PMT, 10 μm slits, and increments of .01 Å (measured peaks rounded to one decimal place for comparison with expected.)

EXPECTED PEAKS(Å)	MEASURED PEAKS(Å)	OFFSET(Å)
5570.3	5571.9	1.6
5870.9	5872.7	1.9
7587.4	7589.3	1.9
7601.5	7603.5	2.0
7685.2	7687.2	2.0
7694.5	7696.4	1.9
7854.8	7856.6	1.8
	Average Offset =	1.9

4) Full width at half maximum (FWHM) with the PMT, 10 μm slits, and increments of .01 Å.

RIGHT λ (Å)	LEFT λ (Å)	DIFFERENCE (Rλ-Lλ)
5572.22	5571.67	.55
5873.00	5872.54	.46
7589.60	7589.09	.51
7603.80	7603.25	.55
7687.46	7686.97	.49
7696.69	7696.18	.51
7856.88	7856.35	.55
	Average FWHM =	.52

The main offset of the silicon detector data has been determined to be due to the inaccuracy of an angle at which one of the mirrors inside the spectrometer was situated.

A second calibration for the change to a grating blazed at 400 nm was done. This was used to correct the spectrometer wavelength readings for the Ti:YAlO fluorescence measurements.

TABLE 2
TABLE OF λ'S FOR 400 NM BLAZE GRATING

1) Main peaks found with the PMT, 10 μm slits, and .2 Å increments.

EXPECTED PEAKS(Å)	MEASURED PEAKS(Å)	OFFSET(Å)
5993.9	5986.0	-7.9
5879.9	5872.0	-7.9
5870.9	5863.0	-7.9
5672.5	5664.4	-8.1
5570.3	5562.2	-8.1
4502.4	4493.8	-8.6
4463.7	4455.2	-8.5
4453.9	4445.4	-8.5
4376.1	4367.6	-8.5
4362.6	4354.2	-8.4
4319.6	4311.0	-8.6
4274.0	4265.6	-8.4
	Average Offset =	-8.3

2) Main peaks found with PMT, 10 μm slits, and 0.1 Å increments.

EXPECTED PEAKS(Å)	MEASURED PEAKS(Å)	OFFSET(Å)
4319.6	4310.9	-8.7
4362.6	4354.2	-8.4
4376.1	4367.8	-8.3
5870.9	5862.9	-8.0
5879.9	5872.0	-7.9
5993.9	5986.1	-7.8
	Average Offset =	-8.2

*U.S.Government Printing Office: 1989 — 748-056/24192